

## Data Acquisition of TiO<sub>2</sub> for Optical Material by using Spectroscopic Ellipsometry Technique

Dr. Asad Sabih Mohammad Raouf \*

Received on:18/1/2010

Accepted on:7/10/2010

### Abstract

An Ellipsometric experimental set up of SOPRA ES4G type with a powerful WVASE software for the theoretical calculus of the Ellipsometry parameters. The Ellipsometry Technique can determine amplitude and phase information  $\Psi$  and  $\Delta$  dependent on wavelength range 250 nm to 900 nm (1.5 - 5 eV), including original practical solutions, were developed. Encouraging results of TiO<sub>2</sub> were obtained in applying the simple Ellipsometric method of azimuths to determine the optical constants for TiO<sub>2</sub> with this optoelectronic device.

**Keywords:** Ellipsometry, Optical properties, Thin film.

### الحصول على البيانات من TiO<sub>2</sub> لمواد بصرية باستخدام تقنيات التحليل الطيفي لمنظومة الألييسوميترية (Ellipsometry)

#### الخلاصة

بأستخدام منظومة سطح القطع الناقص الألييسوميترية (Ellipsometric) المختبرية الجاهزة نو النوع SOPRA ES4G والتي تمتلك خلال أستخدام برنامجها الخاص والمسمى WVASE لحساب التفاضل والتكامل النظري للمعاملات الألييسوميترية Ellipsometry (parameters). ويمكن لتقنية الألييسوميترية (Ellipsometric) تحديد قياسات معلومات السعة والطور ( $\Delta$  و  $\Psi$ ) ضمن مدى طول موجي يتراوح بين 250 - 900 نانومتر (1,5 - 5 اليكترون فولت) وعلى اساس هذه المعلومات قد تم تطوير حلول عملية. أن نتائج البحث كانت مشجعة ومرضية لثنائي أوكسيد التتانيوم TiO<sub>2</sub> وتم الحصول عليها من خلال تطبيق الأسلوب البسيط لسطح القطع الناقص باستخدام الألييسوميترية (Ellipsometric) من السمات لتحديد الثوابت البصرية لثنائي أوكسيد التتانيوم TiO<sub>2</sub> مع هذا الجهاز الأليكترون- بصري ( optoelectronic device ) والمسمى بالألييسوميترية (Ellipsometric) .

### Introduction

Thermal-wave techniques are used for obtaining about the optical and electronic properties variations in semiconductor samples. The most used of these techniques is modulated (or pulsed) photo-reflectance which has been successfully applied to the study

of doping, implantation dose, surface contamination, and carrier diffusion. However all the information contained in the optical reflectivity are not collected from a measurement of reflected absolute intensity; information regarding the polarization state of the reflected electric field is

lost. This additional information can be obtained by an ellipsometry experiment.

Two decade ago the scientists and some research centers presented ellipsometry under pulsed or modulated excitation as new photo-thermal probe [1]. They have transformed a commercial spectroscopic ellipsometry SOPRA ES4G and developed an experimental methodology to realize the measurement of dynamical changes of the ellipsometry parameters induced by an external light excitation [1]. The potential and the sensitivity of the method have been illustrated by measurements performed in time and frequency domains for bulk samples [2] as well as multilayered samples [3].

In the present experimental work, I report a quantitative analysis of experimental results obtained for a TiO<sub>2</sub> bulk sample under pulsed excitation. It was reported that the absolute temperature time evolution can be directly determined from the photoinduced variations of the real and imaginary parts of the refractive index provided by pulsed ellipsometry experiments.

### Theory

Ellipsometry is based on the fact that the polarization of a light beam is altered upon reflection from a bare or film coated surface. An elliptically polarized light beam is defined by the angular position of the ellipse (azimuth), its shape (ellipticity) and the sense of rotation of the light vector. Two parameters determine the state of polarization: these are the

amplitude ratio,  $\text{PSI}(\psi)$ , and the phase difference,  $\text{DELTA}(\Delta)$ .

The reliability of analysis further supported by analyzing the ellipsometric data. Ellipsometry has two main advantages with respect to reflectance measurements: (i) it is less sensitive to the surface roughness and to light-scattering effects; (ii) it allows at each frequency the simultaneous determination of two physical parameters, i. e.,  $n$  and  $k$ .

In the case of bulk samples, this allows the determination of both the real and imaginary parts of the dielectric function without going through a complex treatment analysis. The main drawback with anisotropic samples is that the measured ellipsometric function  $\tan(\psi)$  and  $\cos(\Delta)$  are related both to the incidence angle and the anisotropic reflectance coefficient for polarizations parallel and perpendicular to the incidence plane. The parameters have thus to be deconvolved from a set of measurements performed with different orientations of the sample. Assuming that the anisotropy is uniaxial and that the optical axis of the sample lies on the surface and can be oriented either parallel or perpendicular to the incidence plane, the formalism is simplified and leads to [4, 5]:

$$\tan(\psi^{||,\perp}) \exp(i\Delta^{||,\perp}) = \frac{r_p^{||,\perp}}{r_s^{||,\perp}}, \quad ..(1)$$

$$r_s^{||} = \frac{\cos \phi - \sqrt{(\tilde{n}_\perp^2 - \sin^2 \phi)}}{\cos \phi + \sqrt{(\tilde{n}_\perp^2 - \sin^2 \phi)}}, \quad ..(2)$$

$$r_p^{||} = \frac{\tilde{n}_\parallel \tilde{n}_\perp \cos \phi - \sqrt{(\tilde{n}_\perp^2 - \sin^2 \phi)}}{\tilde{n}_\parallel \tilde{n}_\perp \cos \phi + \sqrt{(\tilde{n}_\perp^2 - \sin^2 \phi)}},$$

$$r_s^\perp = \frac{\cos \phi - \sqrt{(\tilde{n}_\parallel^2 - \sin^2 \phi)}}{\cos \phi + \sqrt{(\tilde{n}_\parallel^2 - \sin^2 \phi)}},$$

$$r_p^\perp = \frac{\tilde{n}_\parallel^2 \cos \phi - \sqrt{(\tilde{n}_\perp^2 - \sin^2 \phi)}}{\tilde{n}_\parallel^2 \cos \phi + \sqrt{(\tilde{n}_\perp^2 - \sin^2 \phi)}}. \quad (3)$$

$r_p^{||,\perp}$  and  $r_s^{||,\perp}$  are the (complex) Fresnel reflection coefficients for light polarized parallel (p) or perpendicular (s) to the incidence plane, respectively, with the optical axis of the sample being parallel ( $\parallel$ ) or perpendicular ( $\perp$ ) to this plane;  $\tilde{n}_\parallel$  and  $\tilde{n}_\perp$  are the complex refractive indices along the extraordinary (parallel to the chains) and ordinary (perpendicular to the chains) axes, respectively;  $\Phi$  is the angle between the normal to the surface of the sample and the direction of propagation of the incident beam. The detector is fixed at the angle  $-\Phi$  in the incidence plane.

On the basis of a couple of ellipsometric measurements performed for the two orientations of the sample at a fixed  $\Phi$  (60°), it is possible numerically invert Eqs.(2) and (3) and extract  $\tilde{n}_\parallel$  and  $\tilde{n}_\perp$ . The complex refractive index determined by ellipsometry is reliable only in the spectral region where the sample can

be considered as a bulk. Below the absorption edge at 2.3 eV, a depolarized light component is superimposed on the ellipsometric signal due to the reflection on the back surface of the sample. This additional component strongly modulates the values of the ellipsometric function, particularly  $\tan(\psi)$ , and affects the spectra at the absorption edge.

### Experimental Details Preparation Method

A pure Titanium substrate with a thermally grown Oxide of nominal thickness of 6nm was used for three samples. The substrate was plasma cleaned by applying 20µs, 4.5kV pulses at a frequency of 1kHz, to the substrate holder, initiating a glow discharge plasma in 5mtorr of Argon gas. The high voltage was then removed and Titanium was deposited using the pulsed cathodic arc. A 99.99% pure Titanium cathode was used with an arc bank voltage of 200V, corresponding to a peak arc current of around 3kA. The arc pulse frequency was set at 0.1Hz and the background gas pressure was less than  $1 \times 10^{-6}$  torr. The magnetic filter was powered using a separate power supply. A deposition rate of around 0.05nm per pulse was expected from previous calibration with a profilomete in order to measure the thickness of TiO<sub>2</sub> samples of 6nm.

### Ellipsometric Measurement

In a conventional ellipsometry experiment, a polarized probe beam is reflected at the sample surface and the change of the polarization state is measured. This measurement is performed through the determination

of a couple of parameters ( $\psi$ ,  $\Delta$ ) or ( $\tan(\psi)$ ,  $\cos(\Delta)$ ) defined by:

$$r_p/r_s = \tan\psi .e^{i\Delta} \dots (4)$$

where  $r_p$  and  $r_s$  are the complex Fresnel reflections coefficients for the electric vector components of the sample for p- (in the plain of incidence) and s-(perpendicular to the plain of incidence) polarized light, respectively.

In Figure (1), the SOPRA ES4G ellipsometry is rotating polarizer - sample - analyzer system that we have adapted in order to perform measurements under unstationary excitation. The experiential procedure is first to fix the azimuth of polarizer (usually 45°), then successively to move the azimuth of the analyzer at four positions (with intervals of 45°) for which the static and the photoinduced signals measured. From these data the ellipsometry parameters  $\tan\psi$ ,  $\cos\Delta$  and their variations  $\delta\tan\psi$ ,  $\delta\cos\Delta$  are determined.

For pulsed excitation, a low power laser (=1mW) is used as probe source to provide a convenient signal to noise ratio. The reflected beam is detected by a fast silicon photodiode (100MHz bandwidth). An Amplifier and a digital oscilloscope working as signal averaging being are used for signal processing. The sensitivity to the relative signal variation is of the order of  $10^{-5}$  with 10MHz detection bandwidth and an average over 1000 shots. As excitation source, the second harmonic of a YAG laser at 0.53 $\mu$ m has been used (pulse of about 3mJ and 30ns). The spot diameters on the

sample surface were 1.2mm for the pump beam and 50 $\mu$ m for the probe.

### Capabilities Of The Wvase Software

The specification of sophisticated analysis of WVASE software programming interface can integrate in Ellipsometric system are:

- Runs under the Microsoft Windows<sup>TM</sup> operating environment: user friendly, supports all output devices that windows<sup>TM</sup> does, copy WVASE data of optical constant parameters ( $\psi$ ,  $\Delta$ ,  $n$ ,  $k$ ,  $\epsilon_i$ ,  $\epsilon_r$ ) against wavelength (in  $\mu$ m or nm) or photon energy in eV to the Windows<sup>TM</sup> clipboard for use in the other Windows<sup>TM</sup> programs.
- Written in C++ and assembly language, for optimum speed.
- Data acquisition capability is integrated with the data analysis software: real-time or off-line process control data analysis capability.
- Packed with features to solve the most complex problems, yet still easy to use for simple data analysis.

### Result And Discussion

Ellipsometric measurements at an incidence angle of 60° have been performed over the spectral range 250 - 900 nm (or 1.5 - 5 eV) on a series of 3 samples as following:

I - (TiO<sub>2</sub>)- Oxidation 700°C 2h + etching alkaline H<sub>2</sub>O<sub>2</sub> 0.5M for 12h

II - (TiO<sub>2</sub>)-Oxidation 700°C 2h + etching

HF/HNO<sub>3</sub>/H<sub>2</sub>O: 1/3/8 for 30 min.

III- (TiO<sub>2</sub>)-Oxidation 700° C 2h.

From Samples I to III shows a smooth, compact surface which at the optical microscope exam appears have a granular structure. Due to the relatively large amount of light diffused by grains and to the large thickness, the material behaves like a bulk sample and no estimate of the layer thickness can be made. A single top layer, 6 nm thick was measured of 50% TiO<sub>2</sub> and 50% voids was added to better account for the surface roughness. This thickness is to some extent arbitrary and simply corresponds to the average thickness obtained from the fits when we leave it as a free parameter; then it was chosen to fix value in order to have a more consistent comparison of the results for the three samples [6]. An evolution was observed in the optical response of the samples when passing from sample I to II and to III. From the Ellipsometric point of view this seems to point towards a better quality of the material (structures becomes progressively larger and better defined as in Figure (2) and Figure (3).

These “bulk” samples are simulated as an effective medium containing TiO<sub>2</sub>, voids, and a small amount of pure Ti. The estimated Ti amount is 6% in sample I and 4% in samples II and III; the void fraction is decreasing from 64 (67) % to 60 (62.4) % passing from I to II and III.

Among the values of the optical functions reported in the literature, the best results in the fit are obtained using the data corresponding to the largest values of the refractive index ( $n \approx 2.25$  at 2 eV). This should indicate a condition of good crystallite of the material. For the sake of comparison we choose of using the functions indicated as TiO<sub>2</sub> in Figure (4) [7].

Some small improvements can be obtained in good mixing some part of Alkaline (H<sub>2</sub>O<sub>2</sub>) with TiO<sub>2</sub> (low index values - slight amorphization) when fitting the data of sample I. The data set TiO<sub>2</sub> has been also used as a basis for the analysis of the thin film samples.

In Figure (5), the various measured Ellipsometry data are presented. We shall consider the first three samples that represent TiO<sub>2</sub> compounds. It was observed that, for TiO<sub>2</sub> compounds, there is a shift towards lower photon energies and the spectra exhibit a “knee” at about 3.8 - 4.15 eV range in the imaginary part  $\epsilon_i$  of the dielectric function Figure (5A). Also the real part of the dielectric function  $\epsilon_r$  in Figure A indicates larger value in the 3.75 - 4.25 eV range. The largest value obtained for TiO<sub>2</sub> from Figure. (5A) is  $\epsilon_i(E_2) \approx (2.5)$  which is nearly half the value reported by Cardona and Greenaway ( $\approx 4.3$ ) by means of reflectivity [5, 8].

This is due to the fact that Ellipsometry deals with intensity independent complex quantities ( $\psi$  and  $\Delta$ ) while reflectance deals with intensities. In addition to that, a power measurement which is very sensitive to intensity fluctuations of the source,

temperature drift of electronic components, macroscopic roughness etc. reflectance measurement has to be taken very accurate since small difference in reflectivity can lead to larger errors in  $\epsilon$  [8, 9].

Figure (3B) Show that the samples of TiO<sub>2</sub> (I,II,III) behavior exhibit a sharp decrease with a minimum  $\psi$  values which is 8.75 PSI in deg at a wavelength near 338 nm for sample I , while it shows 6.45 and 6.4 PSI in deg at wavelength near 370 and 380 nm for samples II and III respectively. The  $\Delta$  values shows a sharp increase with a maximum which is 95 DELTA in deg at a wavelength near 308 nm for sample I , while it shows 120 and 118 DELTA in deg at wavelength near 320 and 325 nm for samples II and III respectively. These behaviors appear that the film thickness deposition is absolutely correct for the pseudodielectric function.

The wavelength region between 275 and 400 nm exhibits considerable changes due to etching method as shown in Figure (5B). It is observed that in sample I curve (etching alkaline) is the best as pseudielectric compared with the samples II and III, and in this case sample I is nearly 50% minimum less influence features than the samples II and III. A smaller change is also observed near 275 nm. When the film thickness is close to the correct thickness and smooth surface due to a chemical treatment (choosing etching chemical) the pseudodielectric function exhibit a smooth transition across the wavelength range and this is not in our case (under investigation for future work) ,as would be expected

for a metallic film in this wavelength region[10,11].

In General for samples of TiO<sub>2</sub> (I,II,III) , one of the obvious features in our work shows there is no noise at longer wavelengths as compared to work of Palik and Nguyen [8,11].

### Conclusions

The results from simulation and experimental were found to be have a strong positive correlation of both  $\psi$  and  $\Delta$  data provide a unique optical model as shown in figures .In the data analysis, the Maquardt-Levenberg [12] algorithm was used to weigh the fitting strength. The objective is to quickly determine the minimum difference or "best fit" between the measured and calculated  $\psi$  and  $\Delta$  values. The (Root) Mean Square Error (MSE) quantifies this difference. The results have a small percentage of difference in the values found for (Root) Mean Square Error (MSE) function commonly used is given by[13],

$$(MSE)^2 = \frac{1}{2N-M} \sum_{i=1}^N \left[ \left( \frac{\psi_i^{mod} - \psi_i^{exp}}{\sigma_{\psi,i}^{exp}} \right)^2 + \left( \frac{\Delta_i^{mod} - \Delta_i^{exp}}{\sigma_{\Delta,i}^{exp}} \right)^2 \right] \dots\dots(5)$$

Where N is the number of measured  $\psi$  and  $\Delta$  pairs, M is the total number of real value fit parameters. Normalization of MSE by the standard deviation of the experimental data  $\sigma_{\psi}^{exp}$  and  $\sigma_{\Delta}^{exp}$  reduces the weight of noisy points.

This is particularly true for the film samples (I, II and III). Anyway some improvements in the best fit procedure can be obtained either by adding some parameter to the model (e.g. by introducing a void fraction also in the

second layer), either by changing the optical function of titanium used in the fit (or using a mix of functions: e.g. a small improvement is obtained by using a low index titanium in the top layer and a high index one in the second layer). Such kinds of changes can affect the results by shifting the equivalent thickness values.

#### References

- [1] G. Jin, J. P. Roger, A. C. Boccara and J.L. Stehle, "Photo Acoustic and Poto- Thermal Phenomena IIP", Springer Series in Optical Sciences , Edited by D. Bicanic, Springer – Verlag, Berlin, 69, P. 474 - 476, (1990).
- [2] G. Jin, H. El Rhaleb, J. P. Roger, A. C. Boccara and J. L. Stehle, "Thin Solid Films", 233 and 234, P. 375-376,(1993).
- [3] G. Jin, H. El Rhaleb, J. P. Roger, A. C. Boccara and J. L. Stehle, J. Phys. D., Appl. Phys. 26 , P. 2096 - 2099, (1993).
- [4] O. S. Heavens, "Optical Properties of Thin Films", Butterworths Scientific, London, (1955).
- [5] S. Logothetidis , " In SITU and Real- Time Spectroscopic Ellipsometry Studies : Carbon Based and Metallic TiNx Thin Films Growth", Handbook of Thin Film Materials, Edited by H.S. Nalwa, Volume 2: "Characterization and Spectroscopy of Thin Films "Copyright 9, 2002 by Academic Press.
- [6] Ana Borrás , Juan R. Sánchez-Valencia , Jesus Garrido - Molinero, Angel Barranco, Agustin R. González – Elipe, "Porosity and Microstructure of Plasma Deposited TiO<sub>2</sub> Thin Films", Microporous and Mesoporous Materials 118: P. 314-324, (2009).
- [7] H. Xie , F.L. Ng and X.T. Zeng , "Spectroscopic Ellipsometry Study of Thin Film Thermo-Optical Properties ",Thin Solid Films, 517: P.5066–5069 , (2009).
- [8] Palik .E.D. Handbook of Optical Constant of Solids, Orlando: Academic Press , (1985).
- [9] E. Masetti, J. Bulir, S. Gagliardi, V. Janicki, A. Krasilnikova, G. Di Santo and C. Coluzza, "Ellipsometric and XPS Analysis of the Interface between Silver and SiO<sub>2</sub>,TiO<sub>2</sub> and SiNx Thin Films", Thin Solid Films 455 - 456, P. 468-472, (2004).
- [10] H. Arain and D. E. Aspnes, "Unambiguous Determination of Thickness and Dielectric Function of Thin Films by Spectroscopic Ellipsometry", Thin Solid Films, 113: P. 101-113, (1984).
- [11] H.V. Nguyen, I. An, and R. W. Collins, Physical Review B, 47(7), P. 3947, (1993).
- [12] W. H. Press, B. P. Flannery, S. A. Teukolsky, and W. T. Vetterling, Numerical Recipes in C, Cambridge University Press, Cambridge, (1988).
- [13] G. E. Jellison, Jr., "Spectroscopic Ellipsometry Data Analysis: Measured Versus Calculated Quantities ", Thin Solid Films, 313-314, P. 33-39, (1998).

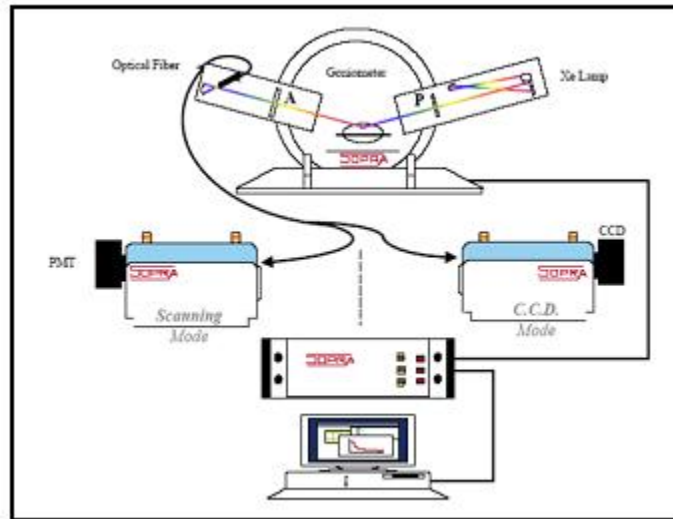
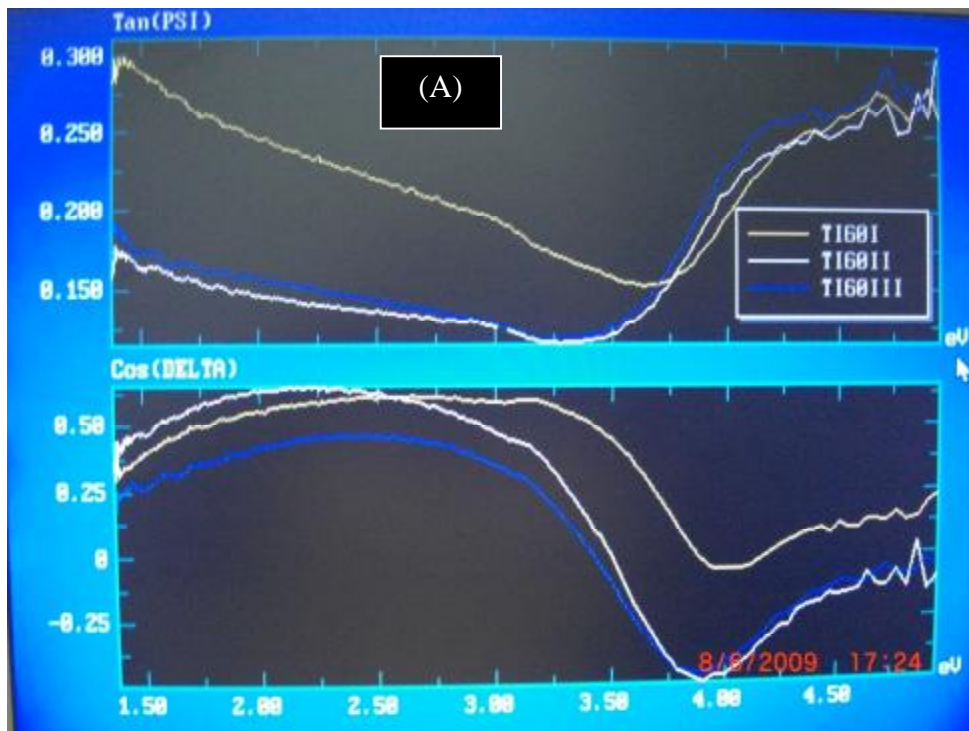


Figure (1) Schematic diagram of Ellipsometer type SOPRA ES4G.





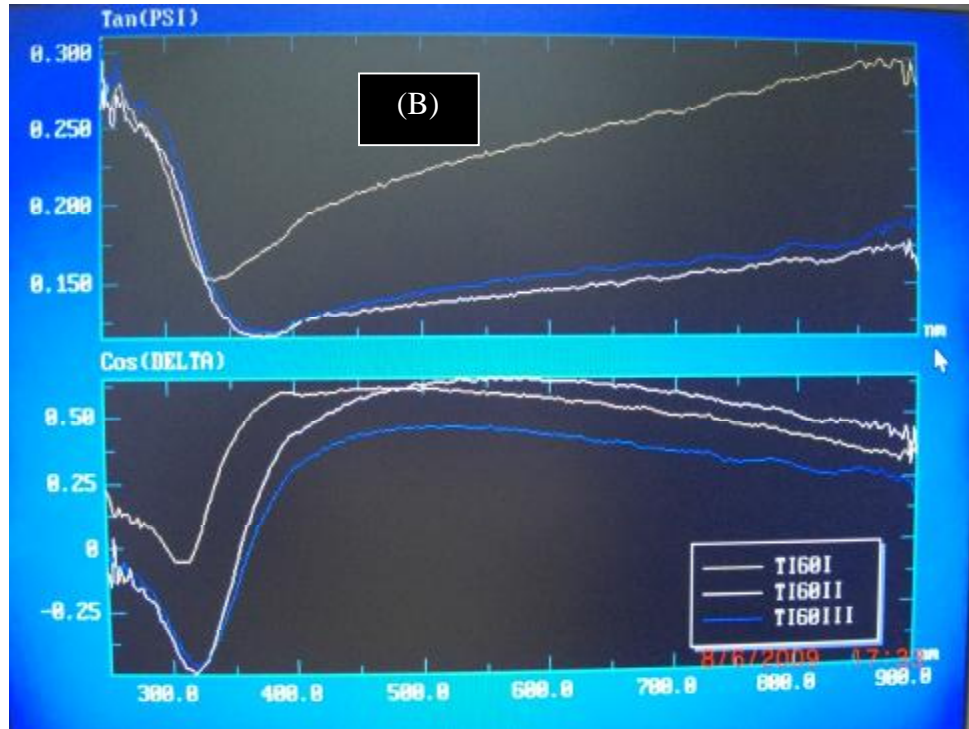


Figure (2): Ellipsometric functions Tan ( $\Psi$ ) and Cos ( $\Delta$ ) measured for the samples I, II and III. (A) As function of Photon Energy (eV); (B) As function of wavelength (nm).

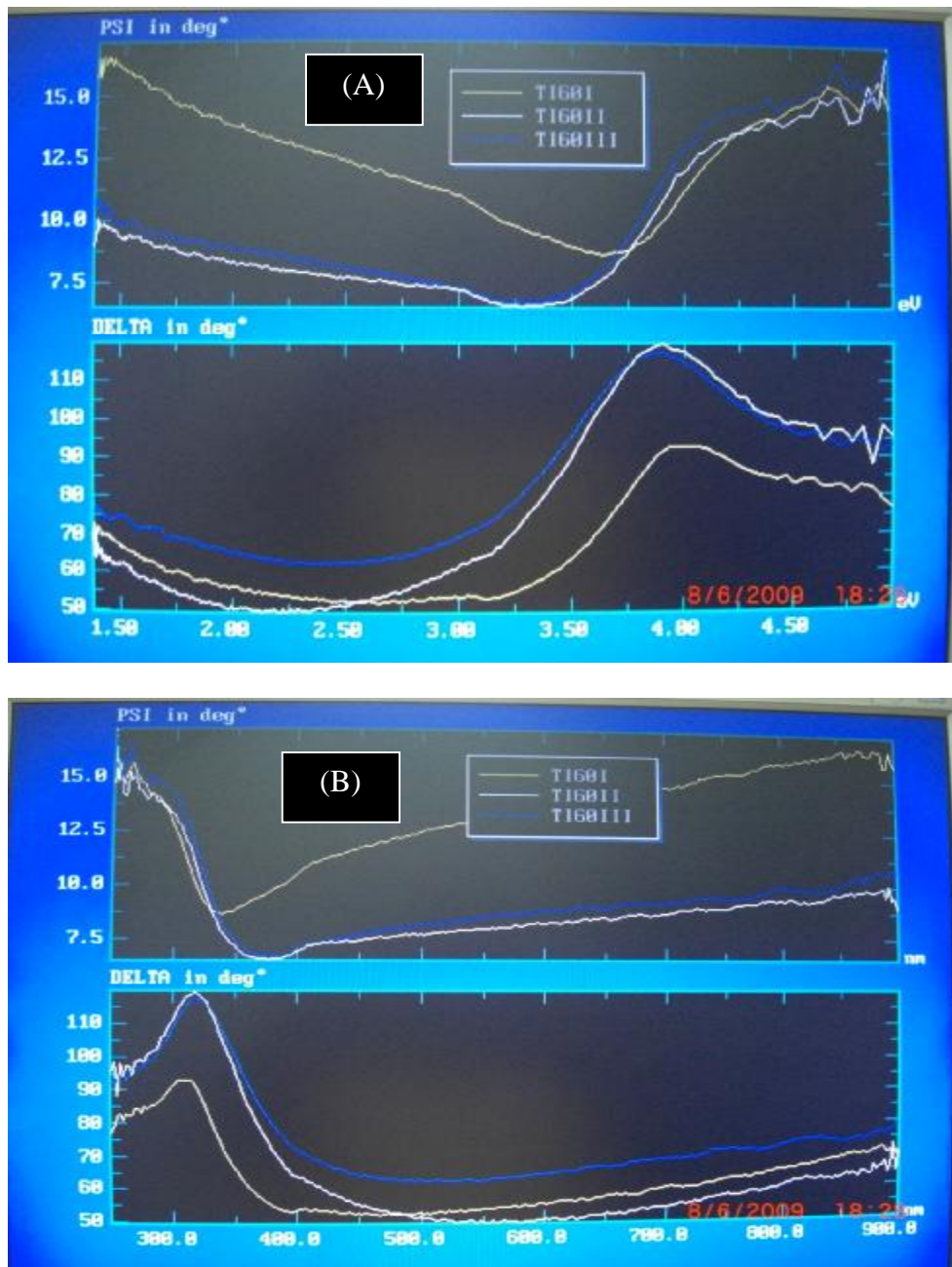


Figure (3) The behaviors of (A) and (B) is the same as in Fig. (2).

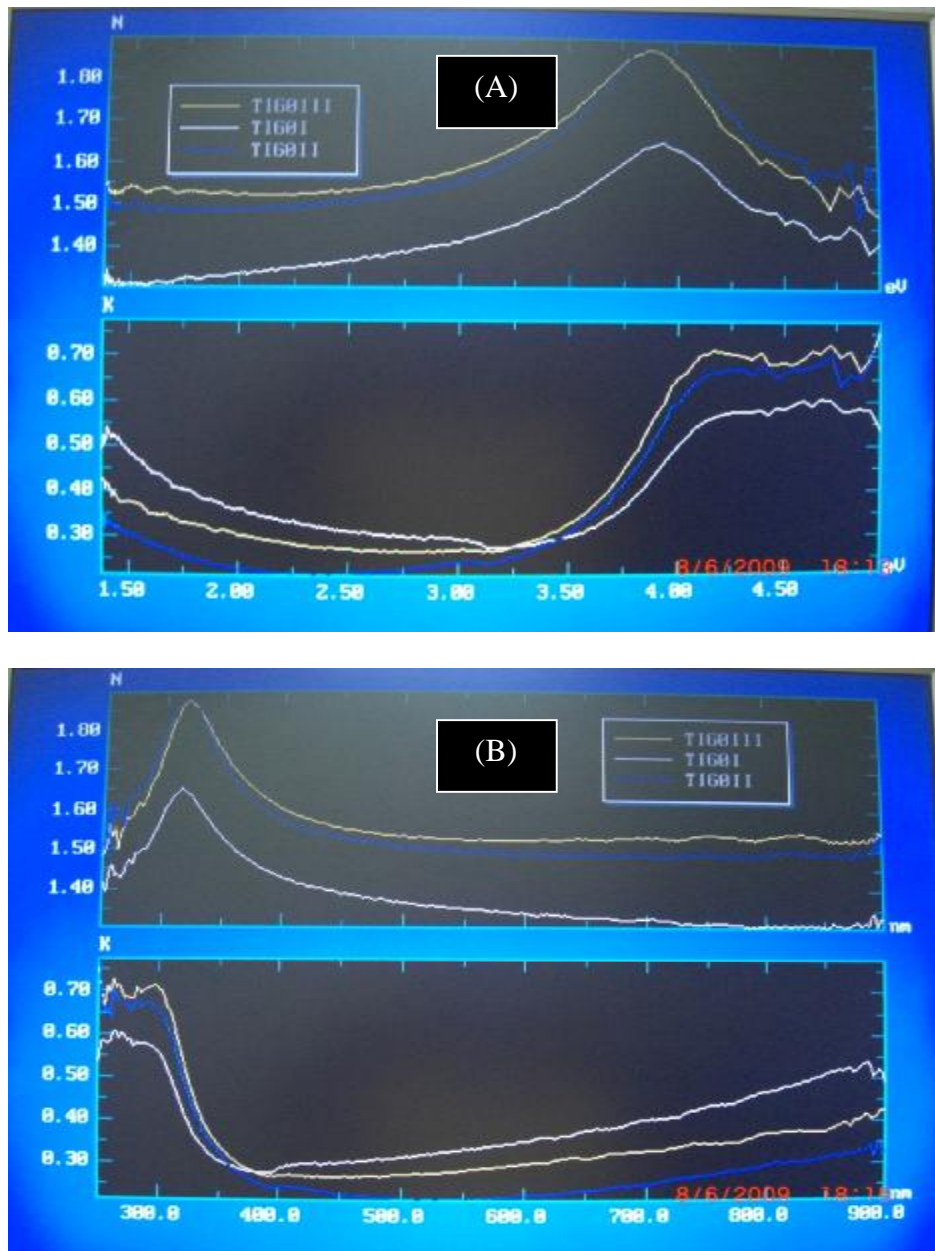


Figure (4): Optical function (refractive index  $n$  and extinction coefficient  $k$ ) of different types of Titanium using the W-VASE software.(A) As function of Photon Energy (eV); (B) As function of wavelength (nm).

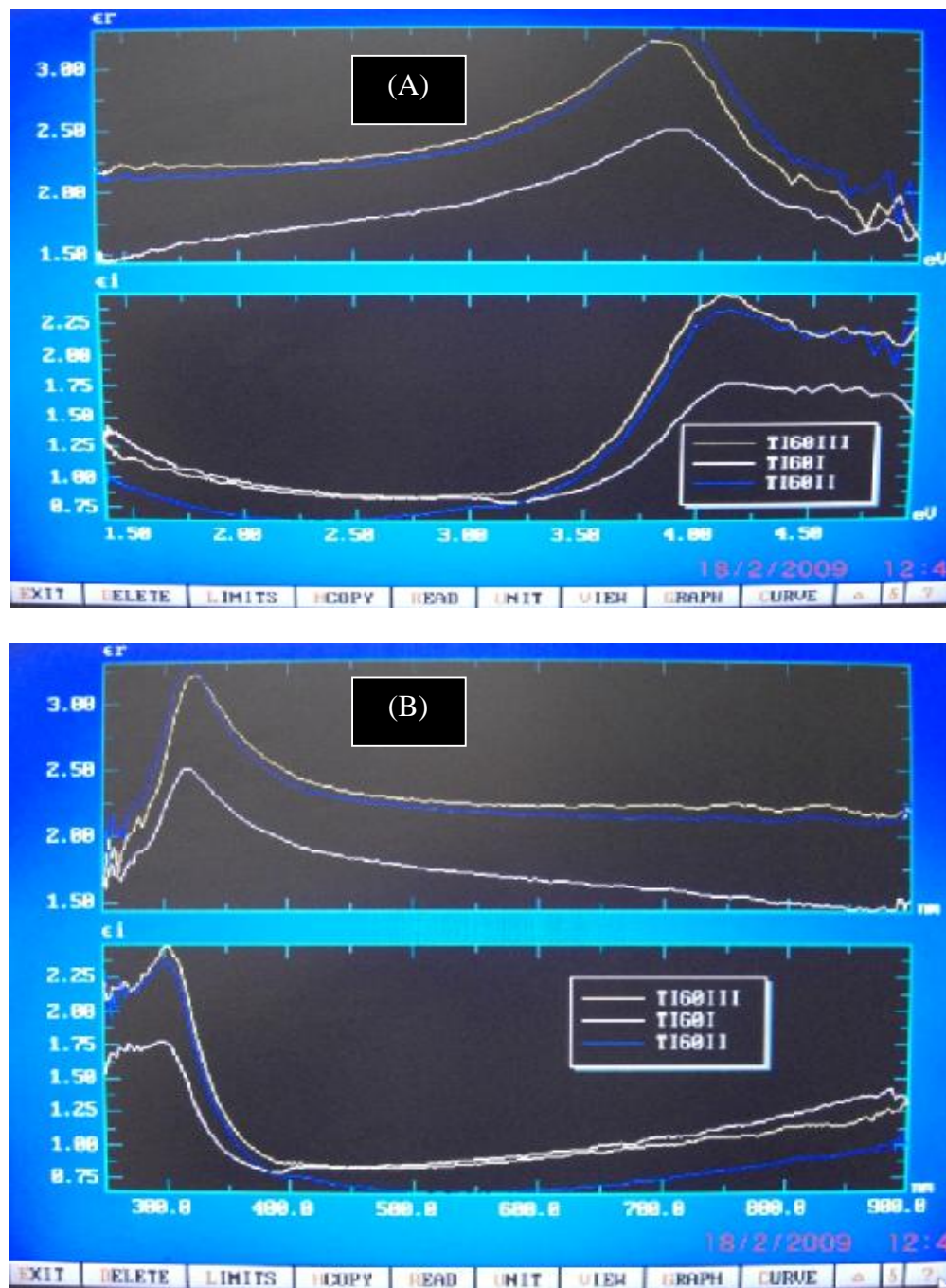


Figure (5): The incident real part and reflected imaginary part.